PHILOSOPHICAL TRANSACTIONS OF THE ROYAL SOCIETY A
MATHEMATICAL, PHYSICAL & ENGINEERING SCIENCES

Classical and Quantum Simulation of the Surface Properties of $\alpha $-Al$_{2}O_{3}$ [and Discussion]

W. C. Mackrodt, John Meurig Thomas and G. Ackland

Phil. Trans. R. Soc. Lond. A 1992 **341**, 301-312
doi: 10.1098/rsta.1992.0103

Classical and quantum simulation of the surface properties of α-Al_2O_3

By W. C. Mackrodt

*ICI Chemicals and Polymers Ltd, PO Box 8, The Heath, Runcorn,
Cheshire WA7 4QD, U.K.*

Classical simulations are described of the fully relaxed surface lattice structures of the five lowest-index planes of α-Al_2O_3 and the resulting crystal morphology. The surface coverage by yttrium and magnesium as a function of temperature is evaluated on the basis of a non-Arrhenius isotherm and calculated heats of surface segregation. The calculated morphology, surface coverages and heats of segregation are compared with experiment. A quantum simulation of a relaxed {0001} surface is presented and the surface structure and energy compared with the classical results. Estimates are made of the adsorption energy of HF at the {0001} surface.

1. Introduction

Oxide surfaces play an important role in a wide range of processes such as catalysis, corrosion, crystal growth, electrolysis and high-temperature superconductivity. However, despite the many advances in surface-sensitive analytic techniques that have occurred over the past decade or so, knowledge of the properties of even the simplest oxide surface remains sparse. For example, reference to the compilation of surface structures by MacLaren *et al.* (1987) reveals that of more than 260 structures cited only ten are for oxides, and then for only six different materials. Experimental surface energies are even more scarce. As elsewhere in solid-state physics and chemistry, computer-based theoretical methods offer a solution to this paucity of information that is increasingly both cost-effective and reliable. Accordingly, to illustrate what is now computationally feasible this paper describes classical and quantum simulations, as these computer-intensive methods are now frequently called, of the surface properties of α-Al_2O_3. α-alumina has been chosen for detailed discussion for a number of reasons: it is a paradigm ceramic with a long history of detailed investigation, though not of its surface properties; classical simulations predict appreciable surface relaxations (Mackrodt 1987), which could be verified directly by techniques such as quantitative I/V low-energy electron diffraction (LEED) and surface X-ray crystallography; there is good data on cation impurity segregation which should be amenable to theoretical interpretation; finally direct comparisons can now be made between classical and quantum simulations.

2. Classical simulations

(*a*) *Theory*

Classical simulations are based on the notion that the total internal potential energy of a system, E, can be written in the form

Phil. Trans. R. Soc. Lond. A (1992) **341**, 301–312

Printed in Great Britain

$$E = \sum_{i,j}{}' e_{ij} + \sum_{i,j,k}{}'' e_{ijk} + \dots, \tag{2.1}$$

in which e_{ij}, e_{ijk} etc are two-, three-, ... n-body terms acting between the constituent particles. Equation (2.1) can be rewritten as

$$E = \sum_{i,j}{}' e_{ij} \{1 + \sum_{k}{}'' e_{ijk}/e_{ij} + \dots\}, \tag{2.2}$$

$$E = \sum_{i,j}{}' \tilde{e}_{ij}, \tag{2.3}$$

with 'effective' two-body potentials, $\tilde{e}_{ij}$, defined as

$$\tilde{e}_{ij} = e_{ij} \{1 + \sum_{k}{}'' e_{ijk}/e_{ij} + \dots\}. \tag{2.4}$$

$\tilde{e}_{ij}$ can be obtained either by fitting analytic forms to known (bulk) properties such as the lattice structure, elastic and dielectric constants and phonon frequencies or by direct calculation using density-functional or Hartree–Fock methods (Catlow *et al.* 1982). All the classical simulations reported here are based on density-functional potentials (Mackrodt & Stewart 1979; Allan *et al.* 1991) which incorporate the shell-model of Dick & Overhauser (1958) to allow for electronic polarization effects (Catlow *et al.* 1982).

The presence of a free surface or any other discontinuity in a crystal, including point defects, leads to a relaxation or distortion of the lattice from the perfect bulk structure. In principle, the relaxation, Q_s, at a surface, s, and the corresponding surface energy, E_s, can be determined from the perfect lattice Green function, G, and the change in the total potential at s, δV_s. For practical purposes, however, the structure (and energy) of the relaxed lattice in the static approximation is more conveniently determined from the condition that the (defective) system is in mechanical equilibrium, i.e.

$$\partial E/\partial X_i = 0, \tag{2.5}$$

where E is the total energy and X_i are all the variables that define the structure. In the case of surfaces, the bulk termination is the most useful reference configuration so that X_i comprise the displacements, Q_s, of the atomic coordinates (and changes in the shell-model polarization) from the bulk positions of atoms/ions in the topmost surface planes. The generality of this approach is such that pure and impure surfaces can be treated in an identical way, which has led to many of the more recent studies on impurity segregation, including those discussed below.

The predominant relaxation is perpendicular to the surface, resulting in a dilation of the surface planes (change in the average separation between them) and rumpling (differential relaxation of unlike atoms/ions in a given plane). Relaxation parallel to the surface is also possible, as shown by Tasker (1984) for the $\{10\bar{1}0\}$ surface of α-Al_2O_3. For most ionic systems, including oxides, relaxation normally decreases fairly rapidly away from the surface, so that in general there is seldom need to relax more than the top five or six planes for simple low-index surfaces. High-index stepped surfaces, on the other hand, frequently require the relaxation of many more planes. The most useful and flexible computer code for calculating the surface structure and energy of ionic materials based on equation (2.1) is the MIDAS code written by Tasker (1978) and the surfaces of a wide variety of ionic crystals have been studied using this.

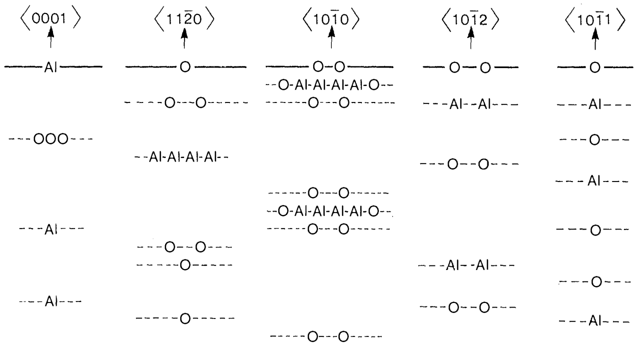

Figure 1. Stacking sequences of the five lowest-index surfaces of α-Al_2O_3.

Table 1. *Classical surface energies* (J m^{-2}) *of* α-Al_2O_3

surface	unrelaxed	relaxed
{0001}	5.95	2.03
{1010}	6.46	2.23
{1012}	3.63	2.29
{1120}	4.37	2.50
{1011}	5.58	2.52

(*b*) *Surface structure*

The surface of α-Al_2O_3 is dominated by the five lowest-index planes, the stacking sequences of which are shown in figure 1. The energies of the unrelaxed surfaces based on electron-gas potentials (Mackrodt 1987) are given in table 1. Thus the relative stability of these surfaces is

$$\{10\bar{1}2\} < \{11\bar{2}0\} < \{10\bar{1}1\} < \{0001\} < \{10\bar{1}0\}$$

in hexagonal notation. Allowing the surfaces to relax to mechanical equilibrium, reduces the surface energies appreciably and changes the order to

$$\{0001\} < \{10\bar{1}0\} \approx \{10\bar{1}2\} < \{11\bar{2}0\} \approx \{10\bar{1}1\},$$

in which the basal surface is now lowest in energy. The corresponding energies are given in table 1. Thus lattice relaxation has three distinct effects. First, it modifies the atomic structure of the surfaces, with changes in lattice spacing of up to 60%, as shown in figure 2 for the {0001} surface. Second, it lowers the individual surface energies by up to a factor of three. Third, it re-orders the relative stability of the surfaces. While there is no direct confirmation as yet for these effects, there is supportive evidence. An approximate value of 0.9 J m^{-2} has been reported for the surface energy of α-Al_2O_3 at 1850 °C (Kingery *et al.* 1976), which presumably represents an average surface energy at this temperature. Following Tasker (1984), the surface energy at a temperature T, $\gamma(T)$, is written in the approximate form

$$\gamma(T) \approx \gamma(0) + \Gamma T, \tag{2.6}$$

from which $\gamma(0)$, the average value at 0 K can be deduced. If, in the absence of a value of Γ for α-Al_2O_3 and as a further approximation, the reported coefficient of -6.3×10^{-4} J m^{-2} K^{-1} for UO_2 (Hodkin & Nicholas 1973) is used, a value of 2.2 J m^{-2} is obtained for $\gamma(0)$. This compares with an unrelaxed average surface

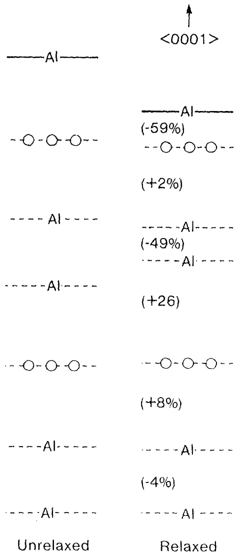

Figure 2. Comparison of the unrelaxed and classically relaxed stacking structure of the {0001} surface of α-Al_2O_3. (Figures in brackets are the percentage changes in the interplanar spacings.)

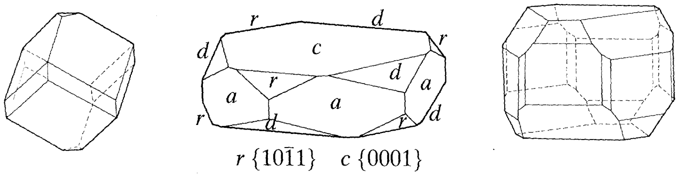

unrelaxed

$r\,\{10\bar{1}1\}$ $c\,\{0001\}$
$d\,\{01\bar{1}2\}$ $a\,\{11\bar{2}0\}$
experimental (Chase 1966)

relaxed

Figure 3. Unrelaxed and relaxed morphologies of α-Al_2O_3 compared with experiment. (Courtesy of the *J. Am. Ceram. Soc.*)

energy of 5.2 J m^{-2} and a value of 2.3 J m^{-2} for fully relaxed surfaces. The relative stability of the individual surfaces may be assessed by invoking the Wulff relation

$$\gamma_i/h_i = \gamma_j/h_j \quad \text{for all} \quad i,j, \tag{2.7}$$

to predict the single-crystal morphology, in which γ_i is the surface energy of surface i and h_i the perpendicular distance of i to a common centre. Figure 3 shows the predicted morphologies for crystals with unrelaxed and relaxed surfaces (Mackrodt *et al.* 1987) compared with an experimental morphology reported by Chase (1966). There is evidently overall agreement between the relaxed and experimental morphologies, particularly in respect of the predominant {0001} face which is barely present in the unrelaxed structure.

(c) {0001} *surface dynamics*

It is possible to go beyond the static approximation and examine the dynamics of alumina surfaces based Cochran's (1977) extension of the lattice dynamics originally due to Born & von Karman (Allan & Mackrodt 1989). Taking the {0001} surface as an example, it is represented by a slab consisting of six fully relaxed stoichiometric units of alumina, i.e. 18 atomic layers. Phonon frequencies are obtained from the

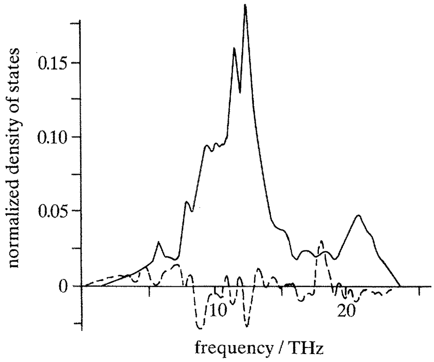

Figure 4. Calculated bulk (——) and surface-excess (– – – – –) phonon densities of states of the {0001} surface of α-Al_2O_3.

eigenvalues of the dynamical matrix which contains both coulombic and non-coulombic contributions. They are extremely sensitive to lattice stability and for lattices which are not at equilibrium, such as the unrelaxed slab, imaginary frequencies are found. The surface-excess phonon density of states is shown in figure 4, together with that for the bulk. The strongest of the surface peaks is predicted at 18 THz, with weaker intensities at approximately 4, 6 and 13 THz. As yet there appears to be no experimental data with which to compare these results.

(*d*) *Impurity segregation*

Ceramics in general, and oxides in particular, can seldom be produced in a completely pure state. Indeed, the presence of impurities is essential to many important processes involving oxides, including catalysis, corrosion and perhaps most notably high T_c superconductivity. Since boundaries of whatever sort provide a different environment from that of the bulk, there is always a free-energy gradient associated with impurities (and other point defects) which drives them to or from a boundary. What simulations can often provide, especially in those cases where experiments are extremely difficult, is information such as changes in surface structure, including the formation of second coherent phases, heats of segregation and equilibrium coverages as a function of temperature and bulk impurity concentration. At thermal equilibrium, the distribution of impurities at a surface is most conveniently described in terms of a segregation isotherm, which is frequently taken to be of the Langmuir or Arrhenius form,

$$[\text{surface}]/[\text{bulk}] = A\exp(-h/k_B T), \tag{2.8}$$

in which [surface] and [bulk] are the surface and bulk concentrations of impurity and h, the heat of segregation, which is assumed to be independent of coverage. However, other than at extremely low coverage this is seldom the case and Mackrodt & Tasker (1989) have derived a more general expression,

$$x_s = x_b \exp\{[s(x_s)+x_s(x_s+1)(\mathrm{d}s(x_s)/\mathrm{d}x_s)]/k_B\} \\ \times \exp\{-[h(x_s)+x_s(x_s+1)(\mathrm{d}h(x_s)/\mathrm{d}x_s)]/k_B T\} \tag{2.9}$$

in which x_s is the ratio of impurity:host ions at the surface and not a concentration. $s(x_s)$ and $h(x_s)$ are the *coverage-dependent* entropy and enthalpy of segregation respectively. They are defined as the differences in the entropy and enthalpy for an isolated atom in the bulk and at the surface. Since the entropic contribution is temperature independent, equation (2.9) can be rewritten as

$$x_{\mathrm{s}} = x_{\mathrm{b}} A' \exp\{-[h(x_{\mathrm{s}}) + x_{\mathrm{s}}(x_{\mathrm{s}}+1)\,(\mathrm{d}h(x_{\mathrm{s}})/\mathrm{d}x_{\mathrm{s}})]/k_{\mathrm{B}}\,T\} \tag{2.10}$$

for direct comparison with equation (2.8). An important difference between equations (2.8) and (2.10) is that whereas H is the slope of ln ([surface]) against $1/k_{\mathrm{B}}\,T$, $h(x_{\mathrm{s}})$ is not equal to the slope of $\ln(x_{\mathrm{s}})$ against $1/k_{\mathrm{B}}\,T$ and cannot be obtained from it. Fortunately, $h(x_{\mathrm{s}})$ can be calculated from lattice simulations. However, before considering two specific examples of impurity segregation, it is worth considering the interpretation of those cases in which there is a linear relation between $\ln(x_{\mathrm{s}})$ and $1/T$.

Rewriting equation (2.6) as

$$\ln(x_{\mathrm{s}}) = \ln(x_{\mathrm{b}} A') - [h(x_{\mathrm{s}}) + x_{\mathrm{s}}(x_{\mathrm{s}}+1)\,(\mathrm{d}h/\mathrm{d}x_{\mathrm{s}})]/k_{\mathrm{B}}\,T\} \tag{2.11}$$

$$= B - H/k_{\mathrm{B}}\,T, \tag{2.12}$$

solutions are sought to the equation

$$h(x_{\mathrm{s}}) + x_{\mathrm{s}}(x_{\mathrm{s}}+1)\,(\mathrm{d}h(x_{\mathrm{s}})/\mathrm{d}x_{\mathrm{s}}) = H, \tag{2.13}$$

where H is a constant.

The equation

$$h(x_{\mathrm{s}}) = H = h \tag{2.14}$$

is clearly the solution when $\mathrm{d}h(x_{\mathrm{s}})/\mathrm{d}x_{\mathrm{s}} = 0$, so that one interpretation of a linear relation between $\ln(x_{\mathrm{s}})$ and $1/T$ is that embodied in the Langmuir–Arrhenius isotherm. The general solution, however, is

$$h(x_{\mathrm{s}}) = H - C(1 + 1/x_{\mathrm{s}}), \tag{2.15}$$

in which C is an undetermined constant. Thus, systems for which $h(x_{\mathrm{s}}) \propto 1/x_{\mathrm{s}}$ will also exhibit Langmuir–Arrhenius behaviour with the possibility that $h(x_{\mathrm{s}})$ and H might be quite different.

Y : Al_2O_3

Yttrium is isovalent with aluminium so that it is a convenient impurity for theoretical study since, to a good approximation, other point defects can be neglected. It is also one of the few cation impurities in alumina for which there is segregation data (McCune *et al.* 1986). In the temperature range 1700 °C to 1900 °C the reported surface coverage of polycrystalline samples is *ca.* 13 % with a heat of segregation of 44 kJ mol^{-1}, although the data are complicated by extensive surface and intergranular precipitation of yttrium aluminium garnet (YAG). Atomistic lattice simulations (Mackrodt 1987) find positive heats of segregation for all but the {0001} surface and highly non-Arrhenius behaviour, as shown in figure 5 for the $\{10\bar{1}2\}$ and $\{11\bar{2}0\}$ surfaces. The values of $h(x_{\mathrm{s}})$ are typically in the range 100–400 kJ mol^{-1}, which is considerably greater than the reported value. The apparent discrepancy between theory and experiment is resolved by comparing the surface coverages. Figure 6 shows that for the $\{10\bar{1}2\}$ and {1120} surfaces, for example, the calculated coverages are very nearly linear in the range 1700–1900 °C, with slopes of -13 and -35 kJ mol^{-1} respectively. These are much more in line with the experimental slope of -44 kJ mol^{-1}, which emphasizes quite clearly the difference between the Arrhenius heat, i.e. the slope of $\ln(x_{\mathrm{s}}/x_{\mathrm{b}})$ against $1/T$, and

Figure 5

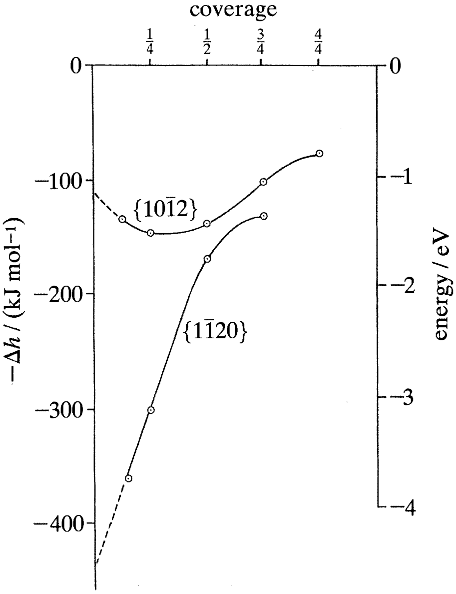

Figure 6

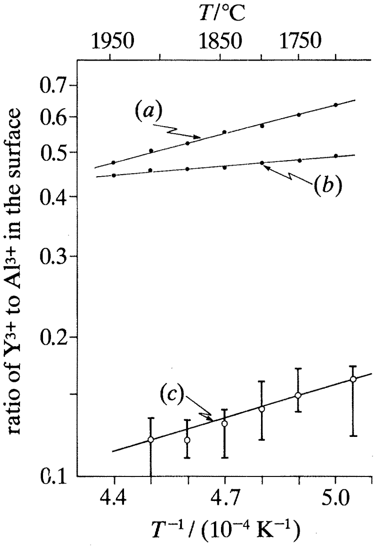

Figure 5. Calculated heat of segregation of yttrium at the {10$\bar{1}$2} and {11$\bar{2}$0} surfaces of α-Al_2O_3.

Figure 6. Calculated (●) and experimental (○) equilibrium coverages of α-Al_2O_3 by yttrium (160 ppm) as a function of temperature. (*a*) {10$\bar{1}$2} surface, $H = -41$ kJ mol^{-1}. (*b*) {11$\bar{2}$0} surface, $H = -13$ kJ mol^{-1}. (*c*) Φ experimental coverage of polycrystalline α-Al_2O_3 (McCune *et al.* 1986), $H = -44$ kJ mol^{-1}.

what might be called the atomic the heat of segregation, $h(x_s)$. There is a discrepancy between the magnitude of the calculated and observed coverages, for which there are essentially three possible reasons. The first is that the very few calculations of the entropy of segregation that have been carried out suggest that A' in equation (2.10) is less than unity. Thus for Ca at {100}MgO the entropy reported by Masri *et al.* (1986) leads to value of 0.9. The second is that the experimental coverage is an average for a finite depth into the crystal which may differ from the surface coverage. The third is that the reported data is for polycrystalline material which is likely to contain a substantial proportion of {0001} surface. Calculations predict negligible segregration to this surface, which, if correct, implies a greater coverage of the other surfaces. Together these suggest closer agreement between theory and experiment than might seem to be case.

Mg: Al_2O_3

The treatment of aliovalent impurities generally is complicated by the need to include the charge compensating defects. In the case of Mg in Al_2O_3 it is believed that oxygen vacancies are the neutralizing species and on this basis the heat of segregation of Mg to the {0001} surface of alumina as the neutral complex, {Mg_{Al}–V_O–Mg_{Al}}, has been calculated (Mackrodt & Tasker 1986): it is shown in figure 7. From zero to about $\frac{1}{4}$ coverage $h(x_s)$ is nearly constant. Beyond this it falls sharply to a minimum at about $\frac{1}{3}$ coverage, after which it rises to a maximum at around $\frac{3}{4}$ coverage. At the minimum value of $h(x_s)$, the ratio of Al^{3+} to Mg^{2+} ions is exactly that of spinel, $MgAl_2O_4$, which suggests the formation of a second coherent phase with this composition at the surface. The corresponding equilibrium coverage is shown in

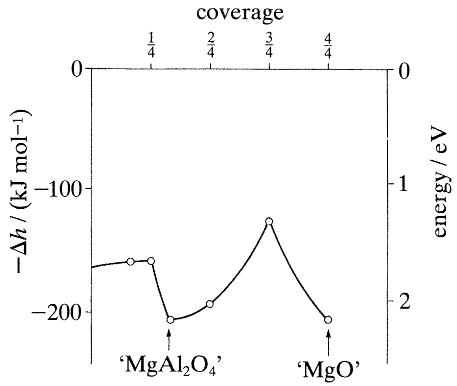

Figure 7. Calculated heat of segregation of magnesium at the {0001} surface of α-Al_2O_3.

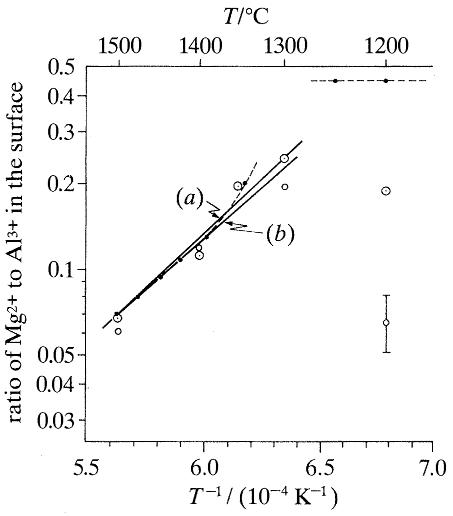

Figure 8. Calculated (●) and experimental (○, 1 *hν*; ⊙, 10 *hν* (Baik *et al.* 1985)) equilibrium coverages of the {0001} surface of α-Al_2O_3 by magnesium (40 ppm) as a function of temperature. (*a*) Experimental, $H = -146$ kJ mol^{-1}; (*b*) calculated $H = -158$ kJ mol^{-1}.

figure 8, together with data reported by Baik *et al.* (1985). Theory and experiment both find Arrhenius-like behaviour up to *ca.* 1370 °C, with slopes that agree to approximately 10 kJ mol^{-1}. Between about 1350 °C and 1250 °C there is a sharp increase in the calculated coverage corresponding to the minimum in $h(x_s)$ and it is not unreasonable to relate the predicted spinel-like second phase to the putative cubic overlayer suggested by the changes in the observed LEED patterns (Baik *et al.* 1985).

3. Quantum simulations

Recent advances in computer technology have made possible a start to the *ab initio* quantum simulation of oxide and other surfaces. Inevitably the size of quantum simulations will be considerably less than classical analogues. However, they will enable direct comparisons to be made in certain cases and beyond this, test some of the assumptions commonly made in classical treatments. For example, classical simulations assume that the charge and polarizability of surface ions and

Table 2. *Quantum simulation of the {0001} surface of alumina*

	ionic charges (Bulk: Al, +2.25; O, −1.50.)	
layer	unrelaxed	relaxed
Al (s)	+1.84	+2.08
O (s−1)	−1.31	−1.39
Al (s−2)	+2.07	+2.10
Al (s−3)	+2.27	+2.26
O (s−4)	−1.50	−1.52

	surface energies ($J\ m^{-2}$)	
	classical	quantum
unrelaxed	5.95	3.20
relaxed	2.03	2.00

	lattice relaxation	
spacing	classical	quantum
s_1	−59%	−49%
s_2	+2%	−5%
s_3	−49%	−8%

the resulting interionic potentials, are essentially that of the bulk. Quantum simulations will allow this to be tested. The quantum methodology used in the examples reported here is the *ab initio* localized orbital Hartree–Fock method (Pisani *et al.* 1988) discussed elsewhere in this volume (Dovesi *et al.* 1992). It has been used to calculate the bulk electronic structure of α-Al_2O_3 (Salasco *et al.* 1991) and the surface features of MgO (Causa *et al.* 1986). The atomic bases used in the simulations reported here (Gale *et al.* 1992) are modifications of the standard 6-21G Pople functions (Binkley *et al.* 1980; Gordon *et al.* 1982). They comprise a 6-21G set for Al and an 8-51G set for O (Dovesi 1985) with the outer exponents of both sets optimized for the experimental bulk structure. This leads to a more ionic structure, than that reported previously, with a Mulliken charge of +2.25 for Al as compared with +1.775 and +2.024 for basis sets with and without Al d-functions (Salasco *et al.* 1991).

(*a*) *{0001} surface structure*

The model for the {0001} surface examined recently by Gale *et al.* (1992) is an infinite two-dimensional slab consisting of up to three stoichiometric units of Al_2O_3 per unit cell, i.e. nine atomic layers perpendicular to the ⟨0001⟩ direction. The unrelaxed surface structure is that of the experimental bulk termination. The Mulliken charge of the surface Al is +1.84 and that of the underlying O is −1.31: these compare with bulk values of +2.25 and −1.50. However, as table 2 shows, the values for third Al layer and second O layer are very close to the bulk charges. The surface energy of the unrelaxed slab is 3.30 $J\ m^{-2}$ compared with the classical value based on electron-gas potentials of 5.95 $J\ m^{-2}$ (Mackrodt 1987). Relaxation of the outer three atomic layers, two Al and one O, leads to an increase in the surface Mulliken charges to +2.08 and −1.39 and a reduction in the surface energy to 2.00 $J\ m^{-2}$ which is close to the classical value of 2.03 $J\ m^{-2}$ (Mackrodt 1987). There

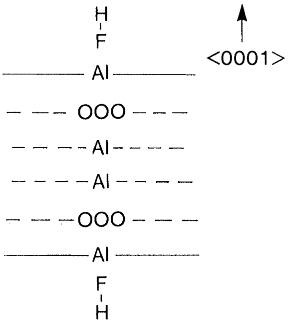

Figure 9. Slab configuration for the quantum simulation of HF adsorbed at the {0001} surface of α-Al_2O_3.

is also good agreement between the surface structures derived from the two methodologies. Classical simulations predict a contraction of the outermost interlayer spacing of 59% compared with a 49% contraction by quantum simulation. Both predict the next spacing to be close to the bulk value with deviations of $+2\%$ and -8% respectively. However, as shown in table 2, there is a difference for the third layer, but this might be due to the fixed inner-most spacing in the quantum simulation.

(*b*) *Sorption of* HF *and* HCl

The use of localized orbitals in the *ab initio* crystal Hartree–Fock approach of Pisani *et al.* (1988) leads to its natural extension to adsorption studies at crystal surfaces (Dovesi *et al.* 1987). Previous calculations of the adsorption energy of CO at {100} MgO found good agreement with experiment for $\frac{1}{2}$ and $\frac{1}{4}$ surface coverage (Dovesi *et al.* 1987). Gale *et al.* (1992) have studied the sorption of hydrogen fluoride at the basal surface of alumina, a process which is relevant to the catalytic fluorination of chlorocarbons (Hedge & Barteau 1989). Their simplest model consists of a fully-relaxed, infinite, two-dimensional slab containing six atomic layers interacting with a single molecule of HF per surface unit cell at both surfaces, as shown in figure 9. It corresponds to a surface coverage of $5.1 \times 10^{-}$ molecules Å^{-2}†. A standard 6-21G basis set was used for HF which leads to an equilibrium bond length of 0.939 Å and dipole moment of 2.15 D, compared with experimental values of 0.917 Å (Kuipers *et al.* 1956) and 1.83 D (Muenter & Klemperer 1970). For the configuration shown in figure 9, the minimum-energy Al–F distance was found to be 1.93 Å, which suggests an essentially long-range interaction between the HF dipole and the electrostatic potential of the surface. At this separation there is an increase in the HF bond length by 0.5% to 0.943 Å and an expansion of the outer-most lattice spacing by about 6%. The binding energy is calculated to be 61.2 kJ mol^{-1} molecule^{-1} with a charge transfer of *ca.* 0.1 e to the surface. Calculations of two-dimensional arrays of HF in the adsorbed configuration indicate that there is a negligible interaction between the HF layers at the two surfaces and a lateral repulsive interaction within each layer of about 20 kJ mol^{-1} molecule^{-1}. This compares with an energy of *ca.* 4 kJ mol^{-1} for the nearest neighbour repulsion. The estimate of the lateral interaction in the adsorbed state is probably low since it does not include the effect of the charge transfer to the surface. However, taken as a first approximation, it leads to an estimate of 81 kJ mol^{-1} for the net binding energy of

---

† 1 Å $= 10^{-10}$ m $= 10^{-1}$ nm.

an HF molecule and the {0001} surface of $-Al_2O_3$. Further calculations of different surface configurations and coverage dependence, which are in progress (Gale *et al.* 1992), should lead to a more reliable value for the binding energy and an estimate of the coverage-dependent heat of adsorption.

References

Allan, N. L. & Mackrodt, W. C. 1989 Calculated surface phonon densities of states of ionic oxides and fluorides. *J. Phys. Condensed Matter* **1**, 189–190.

Allan, N. L., Cooper, D. L. & Mackrodt, W. C. 1991 The practical calculation of interionic potentials in solids using electron gas theory. *Molecular Simulation* **4**, 269–283.

Baik, S., Fowler, D. E., Blakely, J. M. & Raj, R. 1985 Calcium segragation to MgO and α-Al_2O_3 surfaces. *J. Am. ceram. Soc.* **68**, 281–286.

Binkley, J. S., Pople, J. A. & Hehre, W. J. 1980 Self-consistent molecular orbital methods. 21. Small split-valence basis sets for first-row elements. *J. Am. chem. Soc.* **102**, 939–947.

Catlow, C. R. A., Dixon, M. & Mackrodt, W. C. 1982 Interionic potentials in ionic solids. In *Computer simulation of solids* (ed. C. R. A. Catlow & W. C. Mackrodt). Berlin: Springer-Verlag.

Chase, A. B. 1966 Habit modification of corundum crystal grown from molten PbF_2–Bi_2O_3. *J. Am. ceram. Soc.* **49**, 233–236.

Causa, M., Dovesi, R., Pisani, C. & Roetti, C. 1986 *Ab initio* Hartree–Fock structure of the MgO (100) surface. *Surf. Sci.* **175**, 551–560.

Cochran, W. 1977 Lattice dynamics of ionic and covalent crystals. *Crit. Rev. Sol. St. Sci.* **2**, 1–44.

Dick, B. G. & Overhauser, A. W. 1958 Theory of dielectric constants of alkali halide crystals. *Phys. Rev.* **112**, 90.

Dovesi, R. 1985 *Ab initio* Hartree–Fock extended basis set calculation of the electronic structure of crystalline lithium oxide. *Solid State Commun.* **54**, 183–185.

Dovesi, R., Orlando, R., Ricca, F. & Roetti, C. 1987 CO adsorption on MgO crystals: Hartree–Fock calculations for regular adlayers on a (001) lattice plane. *Surf. Sci.* **186**, 267–278.

Dovesi, R., Roetti, C., Freyria-Fava, C., Aprà, E., Saunders, V. R. & Harrison, N. M. 1992 *Phil. Trans. R. Soc. Lond.* A **341**, 203–210.

Gale, J. D., Catlow, C. R. C. & Mackrodt, W. C. 1992 Periodic *ab initio* determination of intermolecular potentials for aluming. *Model. Simulat. Mater. Sci. Engng* (In the press.)

Gordon, M. S., Binkley, J. S., Pople, J. A., Pietro, W. J. & Hehre, W. J. 1982 Self-consistent molecular orbital methods. 22. Small split-valence basis sets for second-row elements. *J. Am. chem. Soc.* **104**, 2797–2803.

Hedge, R. I. & Barteau, M. A. 1989 Preparation, characterisation and activity of fluorinated aluminas for halogen exchange. *J. Catalysis* **120**, 387–400.

Hodkin, E. N. & Nicholas, M. G. 1973 Surface and interfacial properties of stoichiometric uranium dioxide. *J. nucl. Mater.* **47**, 23–30.

Kingery, W. D., Bowen, H. K. & Uhlmann, D. R. 1976 *Introduction to ceramics*, 2nd edn. Wiley.

Kuipers, G. A., Smith, D. F. & Nielsen, A. N. 1956 Infrared spectrum of hydrogen fluoride. *J. chem. Phys.* **25**, 275–279.

Mackrodt, W. C. 1987 The calculated equilibrium segregation of Fe^{3+}, Y^{3+} and La^{3+} at the low-index surfaces of α-Al_2O_3. In *Advances in ceramics*, vol. 23 (ed. C. R. A. Catlow & W. C. Mackrodt), pp. 293–306.

Mackrodt, W. C. & Stewart, R. F. 1979 Defect properties of ionic solids: II Point defect energies based on modified electron-gas potentials. *J. Phys.* C **12**, 431–449.

Mackrodt, W. C. & Tasker, P. W. 1986 Calculated impurity segregation at the surfaces of α-Al_2O_3. *Mater. Res. Soc. Symp. Proc.* **60**, 291–298.

Mackrodt, W. C. & Tasker, P. W. 1989 Segregation isotherms at the surfaces of oxides. *J. Am. ceram. Soc.* **72**, 1576–1583.

Mackrodt, W. C., Davey, R. J., Black, S. W. & Docherty, R. 1987 The morphology of α-Al_2O_3 and α-Fe_2O_3: the importance of surface relaxation. *J. Crystal Growth* **80**, 441–446.

MacLaren, J. M., Pendry, J. B., Rous, P. J., Saldin, D. K., Somorjai, G. A., Van Hove, M. A. & Uvedensky, D. D. 1987 *Surface crystallographic information service: a handbook of surface structures*. Dordrecht: Reidel.

Masri, P., Tasker, P. W., Hoare, J. P. & Harding, J. H. 1986 Entropy and segregation of impurity cations at the surface of an ionic crystal: MgO (001): Ca^{2+}. *Surf. Sci.* **173**, 439–454.

McCune, R. C., Donean, I. N. T. & Ku, R. C. 1986 Yttrium segregation and YAG precipitation at the surfaces of Y-doped α-Al_2O_3. *J. Am. ceram. Soc.* **69**, C196-C199.

Muenter, J. S. & Klemperer, W. 1970 Hyperfine structure constants of HF and DF. *J. chem. Phys.* **52**, 6033–6037.

Pisani, C., Dovesi, R. & Roetti, C. 1988 Hartree–Fock *ab initio* treatment of crystalline systems. *Lecture Notes in Chemistry*, vol. 48. Springer-Verlag.

Salasco, L., Dovesi, R., Orlando, R., Causa, M. & Saunders, V. R. 1991 A periodic *ab initio* extended basis set study of α-Al_2O_3. *Molec. Phys.* **72**, 267–277.

Tasker, P. W. 1978 *A guide to MIDAS*. A.E.R.E. Report R.9130.

Tasker, P. W. 1984 Surfaces of magnesia and alumina. In *Advances in ceramics*, vol. 10 (ed. W. D. Kingery), pp. 176–189.

Discussion

SIR JOHN MEURIG THOMAS (*The Royal Institution, London, U.K.*): Most oxides have hydroxylated surfaces; they seldom end with O^{2-} or M^{2+}. Is the degree of relaxation that you reported for all the prismatic and pyramidal faces (ending in O^{2-} in the idealized state) also seen when you repeat your calculation for α-Al_2O_3 terminating in OH groups?

W. C. MACKRODT: Calculations of the type you refer to have not been carried out for α-Al_2O_3, as far as I am aware. However, similar calculations for MgO indicate that hydroxylation does effect surface relaxation.

G. ACKLAND (*Department of Physics, The University of Edinburgh, U.K.*): The fact that the potential is the same at the bulk and at the surface means that the charge state of the O atom is irrelevant to the relaxation. The Hartree–Fock calculation seems primarily to create O^{2-} ions, and subsequent relaxation is mainly electrostatic and therefore well approximated by the shell model.